DALTON
FULL PAPER

Reaction of *triangulo*-clusters $[Pt_3(\mu\text{-}CO)_3(PR_3)_3]$ with hexafluorobutyne. The X-ray crystal structures of $[Pt_2(CO)_2(PR_3)_2(\mu\text{-}\eta^2\text{:}\eta^2\text{-}CF_3C{\equiv}CCF_3)]$ (PR_3 = PPh_3 or PCy_3) and $[Pt_2(CO)_2(PBzPh_2)(\mu\text{-}\eta^1\text{:}\eta^1\text{-}CF_3C{\equiv}CCF_3)_2]$

Renzo Ros,*[a] Augusto Tassan,[a] Raymond Roulet,*[b] Gàbor Laurenczy,[b] Virginie Duprez[b] and Kurt Schenk[c]

[a] *Dipartimento di Processi Chimici dell'Ingegneria, Via Marzolo 9, I-35131 Padova, Italy*
[b] *Ecole Polytechnique Fédérale de Lausanne, BCH, CH-1015 Lausanne, Switzerland*
[c] *Institut de Cristallographie de l'Université de Lausanne, BSP, CH-1015 Lausanne, Switzerland*

Received 27th March 2002, Accepted 12th July 2002
First published as an Advance Article on the web 20th August 2002

Hexafluoro-2-butyne, $CF_3C{\equiv}CCF_3$, reacts with the *triangulo*-clusters $[Pt_3(\mu\text{-}CO)_3(PR_3)_3]$ to give the diplatinum(0) compounds $[Pt_2(CO)_2(PR_3)_2(\mu\text{-}\eta^2\text{:}\eta^2\text{-}CF_3C{\equiv}CCF_3)]$ {PR_3 = PPh_3 (**1**), $PBzPh_2$ (**2**), PCy_3 (**3**), P^iPr_3 (**4**)}. Spectroscopic properties are reported which are in accord with the molecular structures for **1** and **3**, both having the acetylenic C–C axis perpendicular to the Pt–Pt axis, bridging two $[Pt(CO)(PR_3)]$ fragments in a $\mu\text{-}\eta^2\text{:}\eta^2$ fashion. A large excess of hexafluorobutyne slowly converts **1** and **2** to the diplatinum(II) complexes $[Pt_2(CO)_2(PR_3)_2(\mu\text{-}\eta^1\text{:}\eta^1\text{-}CF_3C{\equiv}CCF_3)_2]$ {PR_3 = PPh_3 (**5**), $PBzPh_2$ (**6**)}, having two planar hexafluorobutyne bridges. This stereochemistry has been established by NMR and IR spectra, and confirmed by single-crystal X-ray diffraction.

Introduction

The ability of hexafluorobutyne (hfb) to coordinate only one metal centre is well known.[1–3] Such complexes are schematically represented as **I** and designated as η^2-acetylene derivatives. Less common are species in which hfb is bonded to two metal centres in a parallel mode (**II**), as in $[Pt_2(\mu\text{-}\eta^1\text{:}\eta^1\text{-}CF_3C{\equiv}CCF_3)(cod)_2]$,[4] or in the perpendicular mode (**III**), as in $[Pt_2(\mu\text{-}\eta^2\text{:}\eta^2\text{-}CF_3C{\equiv}CCF_3)(cod)_2]$ or in the structurally analogous $[Pt_2(\mu\text{-}\eta^2\text{:}\eta^2\text{-}CF_3C{\equiv}CCSiMe_3)(cod)_2]$,[5] formulated on the basis of spectroscopic, analytical, and molecular weight data. The preparation of $[Pt_2(CO)_2(\mu\text{-}CF_3C{\equiv}CCF_3)(\mu\text{-dppm})]$ has been reported,[6] but its structure is not known.

The two alternative geometries **II** and **III**, together with their interconversion energies, have been analysed using qualitative molecular orbital theory.[7]

In the course of our continuing investigation[8,9] into the chemical reactivity of the *triangulo*-complexes $[Pt_3((\mu\text{-}CO)_3(PR_3)_3]$, they were found to react with hexafluorobutyne to give the stable dinuclear derivatives $[Pt_2(CO)_2(PR_3)_2(\mu\text{-}\eta^2\text{:}\eta^2\text{-}CF_3C{\equiv}CCF_3)]$ {PR_3 = PPh_3 (**1**), $PBzPh_2$ (**2**), PCy_3 (**3**), P^iPr_3 (**4**)}, with type **III** structures. Under a large excess of hfb, two of these slowly convert to the diplatinium(II) complexes $[Pt_2(CO)_2(PR_3)_2(\mu\text{-}\eta^1\text{:}\eta^1\text{-}CF_3C{\equiv}CCF_3)_2]$ {PR_3 = PPh_3 (**5**), $PBzPh_2$ (**6**)}. The molecular structures of **1** and **3** have been established by single-crystal X-ray diffraction, and compared with the structurally similar complex $[Pt_2(CO)_2(PCy_3)_2(\mu\text{-}\eta^2\text{:}\eta^2\text{–}^tBuO_2CC{\equiv}CCO_2{}^tBu)]$ recently described.[10] The molecular structure of **6** is also reported, and is the first example of a diplatinum(II) complex having two parallel alkyne bridges.

Results and discussion

Hexafluorobutyne reacts at room temperature with $[Pt_3(\mu\text{-}CO)_3(PR_3)_3]$ in dichloromethane to give the diplatinum(0) compounds $[Pt_2(CO)_2(PR_3)_2(\mu\text{-}\eta^2\text{:}\eta^2\text{-}CF_3C{\equiv}CCF_3)]$ {PR_3 = PPh_3 (**1**), $PBzPh_2$ (**2**), PCy_3 (**3**), P^iPr_3 (**4**)}. In these complexes, the alkyne ligand acts as a 4-electron donor and thereby stabilizes the two 16-electron platinum units, which are structurally analogous to the di(*tert*-butyl)acetylenedicarboxylate derivative $[Pt_2(CO)_2(PCy_3)_2(\mu\text{-}\eta^2\text{:}\eta^2\text{-}{}^tBuO_2CC{\equiv}CCO_2{}^tBu)]$ {PR_3 = PCy_3 (**3**), P^iPr_3 (**4**)}.[10] This binding mode may be identified by its spectroscopic signature. All the dinuclear complexes **1**–**4** are air stable as solids and in solution (their IR and NMR spectra were essentially invariant for a few days). The IR spectrum presents a strong band in the 2012–2030 cm^{-1} region characteristic of terminal CO ligands. All these complexes present only one ^{19}F-NMR resonance, in agreement with the dimeric structure of type **III**, where the CF_3 groups occupy symmetrically equivalent sites (Table 1). For example, the spectrum of **1** (Fig. 1) exhibits five doublets of relative intensity 1:8:17:8:1. This spectrum is the superimposition of the sub-spectra related to the three isotopomers, namely a central doublet due to the $A_3A'_3MM'$ spin system (43.82% abundance, no ^{195}Pt nuclei), which is flanked by two doublets due to the $A_3A'_3MM'X$ spin

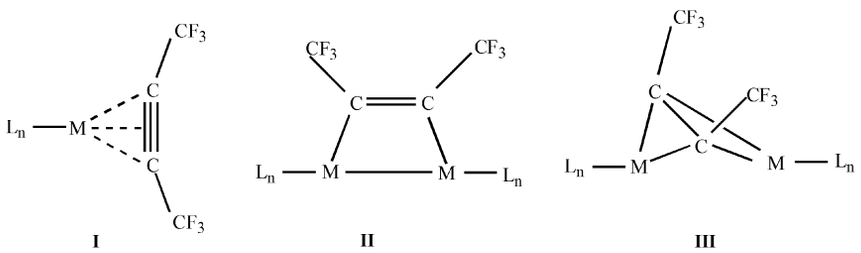

DOI: 10.1039/b203075f

Table 1 Selected ^{19}F-, $^{31}P\{^1H\}$-, and $^{13}C\{^1H\}$-NMR [a] data for complexes **1**–**4** in CD_2Cl_2 at 25 °C (δ/ppm, J/Hz)

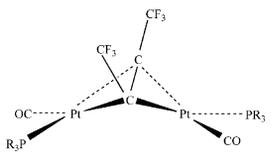

	PR_3			
	PPh_3 (**1**)	PPh_2Bz (**2**)	PCy_3 (**3**)	P^iPr_3 (**4**)
$\delta(F)_{trans}$ [a]	−49.00	−49.69	−48.68	−48.00
$^3J(F–Pt)_{trans}$ [a]	102.8	102.6	97.4	97.3
$^3J(F–Pt)_{cis}$ [a]	102.8	102.6	117.7	115.9
$^4J(F–P)_{trans}$ [a]	13.9	14.0	14.3	14.1
$^4J(F–P)_{cis}$ [a]	< 1	< 1	< 1	< 1
$^5J(F–F)$	~1.2	~1.3	3.4	3.1
$\delta(P)$	16.81	11.95	28.87	42.90
$^1J(P–Pt)$	3351	3356	3191	3222
$^3J(P–Pt)$	−70	−67	−63	−69
$^4J(P–P)$	< 1	< 1	< 1	< 1
$^2J(Pt–Pt)$	382	381	331	341
$\delta(C)$ [b]	182.1	182.9	183.1	183.7
$^1J(C–Pt)$	1658	1656	1632	1633
$^2J(C–P)$	~4.1	~4.4	~4.6	~4.2
$^3J(C–Pt)$	~ −19	~ −18	~ −17	~ −19
$^4J(C–F)_{trans}$ [c]	< 0.7	— [d]	< 0.7	< 0.6

[a] Data for CF_3 groups in pseudo-*trans* and pseudo-*cis* positions relative to PR_3. [b] $^{13}C\{^1H\}$-NMR data for carbonyl ligands of the complexes enriched (>99%) in ^{13}CO. [c] Data for CO groups in pseudo-*trans* positions relative to one CF_3 group. [d] Not observed.

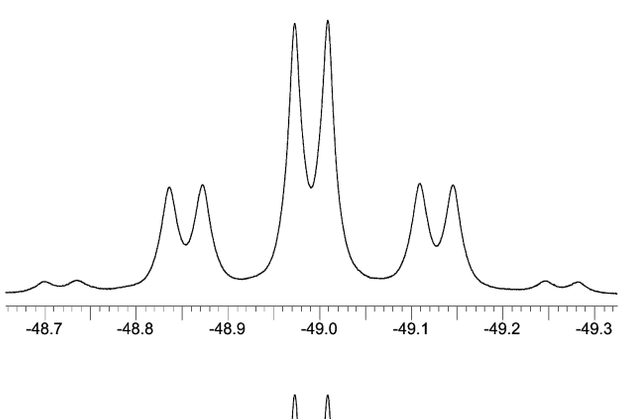

Fig. 1 Observed (top) and simulated (bottom) ^{19}F-NMR spectra of $[Pt_2(CO)_2(PPh_3)_2(\mu\text{-}\eta^2,\eta^2\text{-}CF_3C{\equiv}CCF_3)]$ (**1**) in CD_2Cl_2 at 25 °C.

system (44.75% abundance, one ^{195}Pt nucleus, X), and two external, less intense doublets for the $A_3A'_3MM'XX'$ spin system (11.42% abundance, two ^{195}Pt nuclei, X and X′), with $^3J(Pt–F) = 102.8$, $^4J(P–F)_{trans} = 13.9$, and $^4J(P–F)_{cis} \leq 1$ Hz. In view of their magnitudes, the two P–F coupling are assigned to couplings with the P atoms in pseudo-*trans* positions; pseudo-*cis* P–F couplings could not be detected (< 1 Hz). This result implies two "Pt(CO)(PPh_3)" units symmetrically bridged to the hexafluorobutyne ligand in a $\mu\text{-}\eta^2{:}\eta^2$-fashion. The ^{19}F-NMR spectrum of the $PBzPh_2$ derivative **2** has a very similar pattern (Table 1). The steric bulk of phosphine ligands, such as PCy_3 or P^iPr_3 in **3** and **4**, respectively, renders the two CF_3 groups magnetically non-equivalent, resulting in two multiplets instead of the expected two doublets relative to the isotopomer having one ^{195}Pt (see crystal structures); *i.e.* the two CF_3 groups have two different coupling constants with the neighboring ^{195}Pt atom, together with a small but measurable $^5J(F–F)$. In order to assign these coupling constants, we have collected the $^{19}F\{^{31}P\}$-NMR spectra of compounds **3** and **4** with an adapted Bruker DRX 400 spectrometer. All spectra were satisfactory simulated using the following simplified spin systems: $^{19}F\{^{31}P\}$, $A_3A'_3$ (43.82%, no ^{195}Pt nuclei), $A_3A'_3X$ (44.75%, one ^{195}Pt nucleus), and $A_3A'_3XX'$ (11.42%, two ^{195}Pt nuclei). As an example, the observed and computed spectra of the dimeric cluster **4** are illustrated in Fig. 2.

The $^{31}P\{^1H\}$ and $^{13}C\{^1H\}$-NMR spectra of complexes **1**–**4** are also diagnostic of such a dinuclear geometry. All spectra are consistent with a $Pt_2P_2C_2$ system, where both phosphorous and carbonyl atoms occupy symmetrically equivalent sites, showing a single resonances for these nuclei, with similar patterns of satellites. The rather low values of the $^{195}Pt–^{195}Pt$-coupling constant (331–382 Hz, observed in the ^{31}P spectra) [11–13] rule out any direct metal–metal interaction. Satisfactory computer simulations of these spectra have been achieved on the basis of such a system; for example, the $^{13}C\{^1H\}$-NMR spectral analysis results in the superimposition of the spectra of each of the isotopomers $A_3A'_3MM'NN'$ (43.82%, no ^{195}Pt nuclei), $A_3A'_3MM'NN'X$ (44.75%, one ^{195}Pt nucleus, X), and $A_3A'_3MM'NN'XX'$ (11.42%, two ^{195}Pt nuclei, X and X′). The NMR data for all complexes are summarized in Table 1.

The reaction of hexaflurobutyne (hfb) with $[Pt_3(\mu\text{-}CO)_3(PCy_3)_3]$ (1:1 molar ratio) in toluene was monitored by NMR at −50 °C. No evidence was found of an adduct $[Pt_3(\mu\text{-}CO)_3(PCy_3)_3(\pi\text{-hfb})]$ similar to those observed with olefins. Dimer **3** was observed, together with an isomer of C_s symmetry (obtained by interconverting the positions of P1 and C5 in Fig. 4; δ(CO) 183.4 ppm, J(C–Pt) 1651 Hz, δ(P) 26.8 ppm, J(P–Pt) 3085 Hz). Upon warming the solution to −20 °C, the latter isomer slowly converts to **3**. As one third of a mole of starting trimer is reformed per mole of dimer formed, the final solution shows a **3**:$[Pt_3(CO)_3(PCy_3)_3]$ molar ratio of 1:0.33.

When a large excess of hexafluorobutyne was introduced to a dichloromethane solution of the starting clusters $[Pt_3(\mu\text{-}CO)_3(PR_3)_3]$ (or of the dinuclear intermediates **1** and **2**), a slow declusterization reaction occurred at room temperature. After *ca*. 70 h, total conversion to the scarcely soluble complexes $[Pt_2(CO)_2(PR_3)_2(\mu\text{-}\eta^1{:}\eta^1\text{-}CF_3C{\equiv}CCF_3)_2]$ {PR_3 = PPh_3 (**5**), $PBzPh_2$ (**6**)} was evident, on the basis of their CO frequencies at 2077 and 2078 cm^{-1} respectively, which are characteristic of terminally bonded carbonyl ligands. Their dimeric nature was ascertained by X-ray analysis of **6**, and their formulation as diplatinum(II) complexes is based on the observed square planar arrangement of ligands and on a CO stretching shift *ca*. 40 cm^{-1} to higher wavelengths relative to that observed for the platinum(0) dimers **1** and **2**.

The ^{19}F-NMR spectra of **5** and **6** display two signals of equal intensities which exclude any mirror plane containing the Pt ··· Pt axis or perpendicular to it. The lower field signal (F_{1b}, F_{2a}; Table 2) appears as a doublet of quartets due to $^4J(F–P)$ and $^5J(F–F)$ coupling with ^{195}Pt satellites, whereas the higher field signal (F_{1a}, F_{2b}) is a multiplet due to the additional $^5J(F–P)$ coupling; this assignment is consistent with a lower $^3J(F–Pt)$ according to the greater *trans*-influence of PR_3 relative to CO. The latter pair of CF_3 groups is therefore non-equivalent to the former due to its pseudo-*trans* position with respect to one phosphorous atom. The spectra where simulated successfully using the superposition of three spin systems, $A_3A'_3MM'$, $A_3A'_3MM'X$, and $A_3A'_3MM'XX'$ for the isotopomers with zero, one, and two ^{195}Pt nuclei, respectively. The values of the

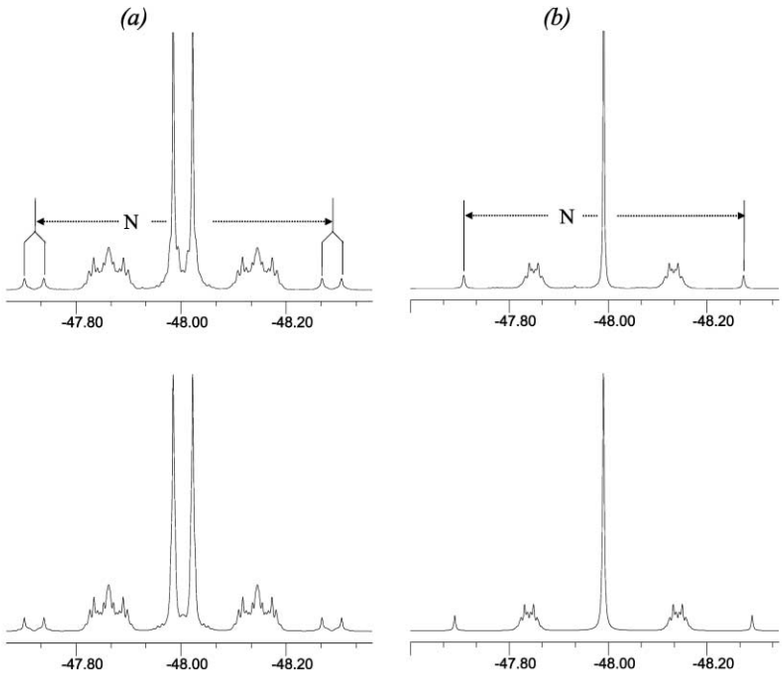

Fig. 2 (a) Observed (top) and simulated (bottom) ^{19}F-NMR spectra of $[Pt_2(CO)_2(P^iPr_3)_2(\mu\text{-}\eta^2,\eta^2\text{-}CF_3C{\equiv}CCF_3)]$ (**4**). (b) The corresponding $^{19}F\{^{31}P\}$-NMR spectra; $N = {}^3J(F\text{–}Pt)_{cis} + {}^3J(F\text{–}Pt)_{trans}$.

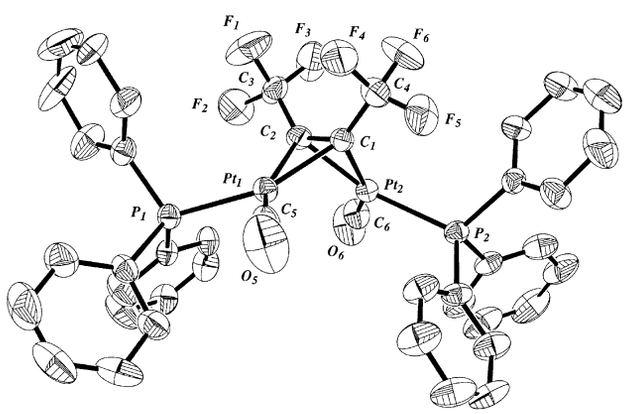

Fig. 3 ORTEP representation at the 40% probability level of one (**1b**) of the two independent molecules of $[Pt_2(CO)_2(PPh_3)_2(\mu\text{-}\eta^2{:}\eta^2\text{-}CF_3C{\equiv}CCF_3)]$ (**1**).

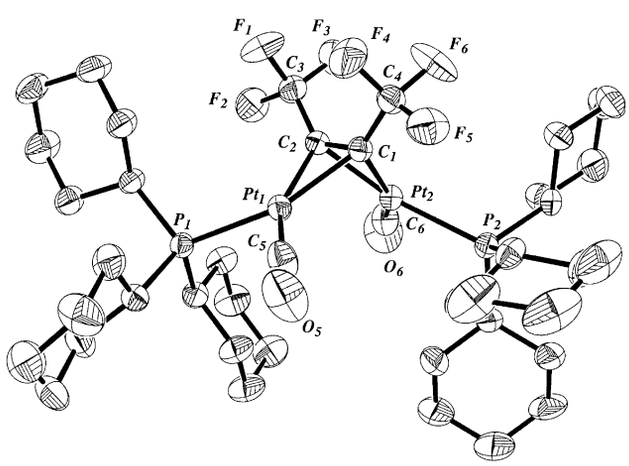

Fig. 4 ORTEP representation at the 40% probability level of complex $[Pt_2(CO)_2(PCy_3)_2(\mu\text{-}\eta^2{:}\eta^2\text{-}CF_3C{\equiv}CCF_3)]$ (**3**).

coupling constants reported in Table 2 were confirmed by selective $^{19}F\{^{31}P\}$ decoupling and selective homonuclear decoupling.

Crystal structures

In order to confirm the structures of both dimeric compound types, single-crystal X-ray crystallographic analyses were completed on **1** and **3**. Details are summarized in the Experimental section. Two independent molecules are present in the crystals of **1** (**1a** and **1b**). Selected intramolecular bond lengths and angles for the molecules are give in Table 3. Views of the molecules **1b** and **3** are presented in Fig. 3 and 4, respectively. The atoms coordinated to platinum deviate slightly from planarity: the values for the angle between the plane defined by C(2), C(1), Pt(1) and Pt(1), P(1), C(5) are 1.3, 4.2, and 7.5° for **3**, **1a**, and **1b**, respectively. The corresponding values for the planes at Pt(2) are 2.9, 6.0, and 6.7° for **3**, **1a**, and **1b**, respectively. The hexafluorobutyne has been perturbed considerably on coordination. The acetylenic bond lengths of 1.417(6) (mean) and 1.401(4) Å for **1a**, **1b**, and **3**, respectively are larger than the values of 1.255(9), 1.260(10), and 1.282(9) Å observed in the zerovalent platinum compounds $PtL_2(CF_3C{\equiv}CCF_3)$ L = PPh_3,[14] PCy_3,[15] and $AsPh_3$,[16] respectively, and significantly larger than the average value of 1.202(5) Å found in free acetylenes.[17] Likewise, the mean values for the acetylenic bend-back angle are significantly greater (47.4, 46.7, and 48.0° for **1a**, **1b**, and **3**, respectively) than the corresponding values for $PtL_2(CF_3C{\equiv}CCF_3)$ (39.9 and 45.4° for L = PPh_3 and PCy_3, respectively), probably because the acetylenic carbon atoms are bonded to two metal atoms. No correlation could be found between the Pt–C–C–F dihedral angles and the coupling constants reported in Table 1.

In order to confirm the dimeric nature of the products of the reaction of the starting clusters with a large excess of hexafluorobutyne, a single-crystal X-ray crystallographic analysis was completed on $[Pt_2(CO)_2(PBzPh_2)_2(\mu\text{-}\eta^1{:}\eta^1\text{-}CF_3C{\equiv}CCF_3)_2]$ (**6**). Details are summarized in the Experimental section. Selected intramolecular bond lengths and angles for the molecules are give in Table 3. The molecular structure of **6** is illustrated in Fig. 5. As expected from the NMR data, two molecular $Pt(CO)(PBzPh_2)$ fragments are present in the structure, both σ-bonded symmetrically by two hexafluorobutyne ligands. The C(1a)–C(2a) and C(1b)–C(2b) separations of 1.316(5) and 1.303(5) Å, respectively, and the angles about C(1a), C(2a), C(1b), and C(2b) suggest that the hybridization of these atoms is close to sp^2. The Pt(II)–C(sp^2) distances in **6**

Table 2 Selected NMR data for **5** and **6** in CD_2Cl_2 at 25 °C (δ/ppm, J/Hz)

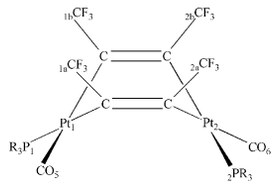

			F_{2a}	F_{1b}	P_1	P_2	Pt_1	Pt_2
Complex **5**								
$\delta(F_{1a,\ 2b})$	−54.66	F_{1a}	12.6		8.8	3.9	123.9	~6
$\delta(F_{1b,\ 2a})$	−52.53	F_{2b}		12.6	3.9	8.8	~6	123.9
$\delta(P_{1,\ 2})$	8.87	F_{1b}			1.5		130.0	~10
		F_{2a}				1.5	~10	130.0
$\delta(CO_{5,\ 6})$	174.8[a]	P_1					1949	
		P_2						1949
Complex **6**								
$\delta(F_{1a,\ 2b})$	−54.80	F_{1a}	13.3		8.9	4.1	122.5	~6
$\delta(F_{1b,\ 2a})$	−51.56	F_{2b}		13.3	4.1	8.9	~6	122.5
$\delta(P_{1,\ 2})$	12.77	F_{1b}			2.2		130.2	~9
		F_{2a}				2.2	~9	130.2
$\delta(CO_{5,6})$	173.5[a]	P_1					2001	
		P_2						2001

[a] $^1J(CO_5–Pt_1) = {}^1J(CO_6–Pt_2)$ 1113, 1106; $^2J(CO_5–P_1) = {}^2J(CO_6–P_2)$ ~4.4, ~3.9; $^4J(CO_5–F_{1b}) = {}^4J(CO_6–F_{2a})$ ~3.2, ~3.7 for **5** and **6**, respectively.

Table 3 Selected bond lengths [Å] and angles [°] for **1**, **3**, and **6**

	1a	**1b**	**3**	**6**[a]
Pt(1)–Pt(2)	3.056(1)	3.096(1)	3.068(1)	3.218(1)
Pt(1)–P(1)	2.304(1)	2.315(1)	2.337(1)	2.339(1)
Pt(1)–C(5)	1.905(5)	1.892(5)	1.872(5)	1.936(4)
Pt(1)–C(1)	2.069(4)	2.063(4)	2.068(3)	(a) 2.086(3), (b) 2.092(3)
Pt(1)–C(2)	2.065(4)	2.053(4)	2.069(3)	
Pt(2)–P(2)	2.311(1)	2.307(1)	2.329(1)	2.335(1)
Pt(2)–C(6)	1.885(4)	1.904(4)	1.873(4)	1.917(4)
Pt(2)–C(1)	2.056(3)	2.059(4)	2.063(3)	
Pt(2)–C(2)	2.098(3)	2.072(4)	2.069(3)	(a) 2.075(3), (b) 2.085(4)
C(1)–C(2)	1.416(6)	1.418(5)	1.401(4)	(a) 1.316(5), (b) 1.303(5)
C(2)–C(3)	1.450(6)	1.469(6)	1.468(5)	(a) 1.500(5), (b) 1.509(5)
C(1)–C(4)	1.479(6)	1.474(5)	1.471(5)	(a) 1.487(5), (b) 1.495(5)
C(5)–O(5)	1.118(6)	1.109(6)	1.143(5)	1.104(4)
C(6)–O(6)	1.125(5)	1.096(5)	1.140(4)	1.126(5)
Pt(1)–C(1)–C(2)	69.8(2)	69.5(2)	70.3(2)	(a) 116.8(2), (b) 117.6(3)
Pt(1)–C(1)–Pt(2)	95.6(2)	97.4(1)	95.9(1)	
Pt(1)–C(1)–C(4)	128.7(3)	129.1(3)	128.8(2)	(a) 115.5(2), (b) 118.4(3)
Pt(2)–C(1)–C(4)	132.8(3)	131.1(3)	133.3(3)	
C(1)–C(2)–Pt(2)	68.5(2)	69.4(2)	69.9(2)	(a) 117.6(3), (b) 116.9(3)
Pt(1)–C(2)–Pt(2)	94.4(2)	97.3(2)	95.7(1)	
Pt(1)–C(2)–C(3)	133.9(3)	132.4(3)	70.1(2)	
Pt(2)–C(2)–C(3)	129.7(3)	128.3(3)	128.2(3)	(a) 118.6(3), (b) 115.9(2)
C(5)–Pt(1)–P(1)	98.1(1)	99.2(1)	97.5(1)	91.1(1)
C(1)–Pt(1)–C(2)	40.0(2)	40.3(2)	39.6(1)	
C(5)–Pt(1)–C(1)	114.7(2)	112.8(2)	112.6(2)	(a) 90.3(2), (b) 173.2(1)
P(1)–Pt(1)–C(2)	107.1(1)	107.4(1)	110.3(1)	
Pt(1)–C(5)–O(5)	177.4(4)	175.6(6)	178.8(5)	178.1(3)
C(6)–Pt(2)–P(2)	100.1(1)	100.5(2)	97.5(1)	92.9(1)
C(1)–Pt(2)–C(2)	39.8(2)	40.1(2)	39.6(1)	
C(6)–Pt(2)–C(2)	113.4(2)	111.1(2)	113.4(2)	(a) 173.6(2), (b) 90.3(2)
P(2)–Pt(2)–C(1)	106.8(1)	108.2(1)	109.4(1)	
Pt(2)–C(6)–O(6)	179.4(4)	176.7(5)	178.6(4)	176.7(4)
C(1)–C(2)–C(3)	132.4(4)	132.9(4)	132.5(3)	(a) 123.8(3), (b) 127.2(3)
C(2)–C(1)–C(4)	132.9(4)	133.7(4)	131.4(3)	(a) 127.7(3), (b) 123.9(3)
P(1)–Pt(1)–C(1)	146.6(1)	147.5(1)	149.90(9)	(a) 178.6(1), (b) 94.8(1)
P(2)–Pt(2)–C(2)	146.2(1)	148.4(1)	149.07(9)	(a) 93.4(1), (b) 176.8(1)

[a] The letters a and b refer to the two hexafluorobutyne bridges (see Fig. 5).

[average 2.085(4) Å] are normal for σ-bonds.[18] The Pt(1)–Pt(2) separation of 3.218(1) Å is more than twice the covalent radius of platinum, as found in $[Pt_2(CO)_2(PBzPh_2)_2(\mu\text{-}\eta^1,\eta^1\text{-}{}^t\!BuO_2CC{\equiv}CCO_2{}^t\!Bu)]$ {2.638(8) Å},[10] and is comparable with the Pt–Pt separations of 3.056(1)–3.096(1) Å in **1** and **3**, in which the μ-η²,η²-alkyne ligand prevents direct Pt–Pt bonding. In compound **6**, the two platinum atoms have a 16-electron configuration and planar coordination [the mean deviations of the

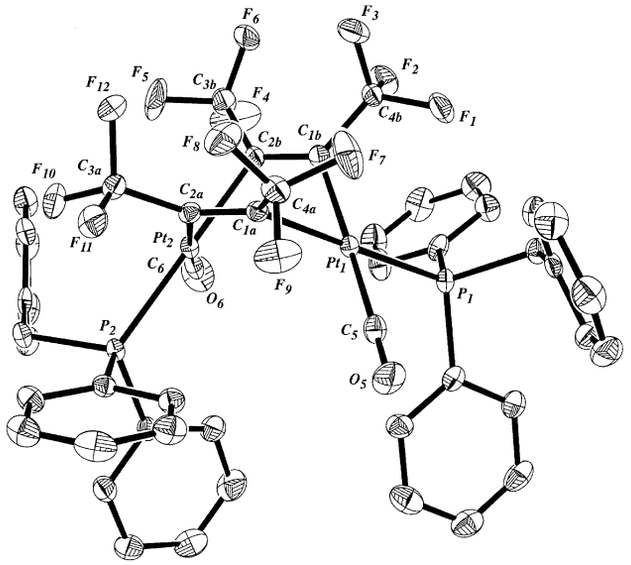

Fig. 5 ORTEP representation at the 30% probability level of $[Pt_2(CO)_2(PR_3)_2(\mu\text{-}\eta^1\text{:}\eta^1\text{-}CF_3C{\equiv}CCF_3)_2]$ (**6**).

coordinated atoms from the planes containing Pt(1) and Pt(2) are 0.029 and 0.013 Å, respectively]; the interplanar angle is 82.8(1)°.

Experimental

General procedures

All manipulations were carried out under nitrogen atmospheres using standard Schlenk techniques. All solvents were dried by conventional methods and distilled prior to use.

Infrared spectra of solids (KBr, Nujol mulls) and CH_2Cl_2 solutions (KBr or CaF_2 cells) were recorded on Perkin-Elmer 983 or FT-IR-2000 spectrometers, and NMR spectra on Bruker AC 200 (^{1}H at 200.13 MHz, ^{31}P at 81.02 MHz, and ^{13}C at 50.32 MHz), Bruker WH 360 (^{13}C at 90.55 MHz), or Bruker DRX 400 (^{31}P at 161.93 MHz, ^{13}C at 100.6 MHz, and ^{19}F at 376.4 MHz) spectrometers. The chemical shifts (δ) are referred to Me_4Si (^{1}H and ^{13}C), $CFCl_3$ (^{19}F) or external 85% H_3PO_4 (^{31}P), respectively. The spectra of all nuclei (except ^{1}H) were ^{1}H decoupled. Simulations were performed with the gNMR 4.0 program, taking into account only the relative population of platinum isotopomers, since all samples for $^{13}C\{^1H\}$-NMR were enriched to ≥99% ^{13}CO.[8] Microanalyses were obtained from the Department of Inorganic, Metalorganic and Analytical Chemistry, University of Padova.

The compounds $[Pt_3(CO)_3(PR_3)_3]$, where L = PPh_3,[8] $PBzPh_2$,[8,19] PCy_3,[20] and P^iPr_3[20] were prepared by literature methods. The ^{13}C isotopically labeled derivatives were prepared similarly, using ^{13}CO enriched to 99%. Hexafluoro-2-butyne (Aldrich) and carbon monoxide (> 99% ^{13}CO) were used as received.

Syntheses

$[Pt_2(CO)_2(PPh_3)_2(\mu\text{-}\eta^2\text{:}\eta^2\text{-}CF_3C{\equiv}CCF_3)]$ (1). A suspension of $[Pt_3(CO)_3(PPh_3)_3]$ (0.29 g, 0.20 mmol) in a 1:2 dichloromethane–heptane mixture (25 ml) was cooled to −10 °C and gaseous $CF_3C{\equiv}CCF_3$ (15 ml, 0.62 mmol) was added with a syringe. The mixture was stirred for 10 min at this temperature and then 1 h at room temperature. Concentration of the resulting solution, followed by addition of heptane and cooling overnight at −22 °C gave a whitish solid. Recrystallization from dichloromethane–isopropanol at low temperature afforded **1** as ivory crystals suitable for X-ray diffraction studies (Yield: 0.251 g, 74%). M.p. 163–166 °C dec. (Found: C, 44.53; H, 2.67; $C_{42}H_{30}F_6O_2P_2Pt_2$ requires C, 44.80; H, 2.65%). Selected IR data (cm^{-1}): CH_2Cl_2 solution ν(C≡O) 2031vs; Nujol mull $\nu(CF)_{sym}$ 1276s, $\nu(CF)_{deg}$ 1172s, 1121s, 1099s.

$[Pt_2(CO)_2(PBzPh_2)_2(\mu\text{-}\eta^2\text{:}\eta^2\text{-}CF_3C{\equiv}CCF_3)]$ (2). Prepared as for **1**, starting with $[Pt_3(CO)_3(PBzPh_2)_3]$ (0.27 g, 0.18 mmol) and $CF_3C{\equiv}CCF_3$ (20 ml, 0.83 mmol). Yield: 0.198 g (63%) as ivory crystals after crystallization from dichloromethane–heptane. M.p. 102–107 °C dec. (Found: C, 45.85; H, 3.03; $C_{44}H_{34}F_6O_2P_2Pt_2$ requires C, 45.52; H, 2.95%). Selected IR data (cm^{-1}): CH_2Cl_2 solution ν(C≡O) 2029vs; Nujol mull $\nu(CF)_{sym}$ 1275s, $\nu(CF)_{deg}$ 1168s, 1118s, 1098s.

$[Pt_2(CO)_2(PCy_3)_2(\mu\text{-}\eta^2\text{:}\eta^2\text{-}CF_3C{\equiv}CCF_3)]$ (3). A suspension of $[Pt_3(CO)_3(PCy_3)_3]$ (0.332 g, 0.22 mmol) in dichloromethane (20 ml) was cooled at −20 °C and gaseous $CF_3C{\equiv}CCF_3$ (25ml, 1.04 mmol) was added. The suspension was stirred for 10 min at this temperature and then at room temperature. After 1 h, the pale orange solution obtained was concentrated under vacuum to *ca*. 2 ml. Addition of pentane (10 ml) and cooling at −22 °C overnight afforded pale grey crystals of **3**. Recrystallization from dichloromethane–heptane at low temperature gave ivory crystals suitable for X-ray diffraction studies (Yield: 0.251 g, 65%). M.p. 201–204 °C dec. (Found: C, 43.15; H, 5.60; $C_{42}H_{66}F_6O_2P_2Pt_2$ requires C, 43.15; H, 5.69%). Selected IR data (cm^{-1}): CH_2Cl_2 solution ν(C≡O) 2012vs; Nujol mull $\nu(CF)_{sym}$ 1272s, $\nu(CF)_{deg}$ 1167s, 1109s, 1103s.

$[Pt_2(CO)_2(P^iPr_3)_2(\mu\text{-}\eta^2\text{:}\eta^2\text{-}CF_3C{\equiv}CCF_3)]$ (4). A solution of $[Pt_3(CO)_3(P^iPr_3)_3]$ (0.437 g, 0.38 mmol) in dichloromethane (15 ml) was cooled at −20 °C and gaseous $CF_3C{\equiv}CCF_3$ (37 ml, 1.54 mmol) was added. After 30 min at room temperature, the pale orange solution was evaporated to dryness and crude **4** was treated with 5 ml of cold pentane. The ivory–ochre solid was filtered and recrystallized from dichloromethane–heptane at −22 °C overnight (Yield: 0.292 g, 55%). Selected IR data (cm^{-1}): CH_2Cl_2 solution ν(C≡O) 2016vs; Nujol mull $\nu(CF)_{sym}$ 1274s, $\nu(CF)_{deg}$ 1165s, 1109s, 1100s.

$[Pt_2(CO)_2(PPh_3)_2(\mu\text{-}\eta^1\text{:}\eta^1\text{-}CF_3C{\equiv}CCF_3)_2]$ (5). A solution of $[Pt_3(CO)_3(PPh_3)_3]$ (0.195 g, 0.134 mmol) in dichloromethane (25 ml) was cooled at −20 °C and gaseous $CF_3C{\equiv}CCF_3$ (55 ml, 2.29 mmol) was added. After 10 min at this teperature, the solution was stirred at room temperature for 70 h. Concentration of the resulting suspension to few ml, followed by addition of heptane (20 ml), gave a whitish solid. Recrystallization from dichloromethane–heptane at low temperature afforded **5** as ivory microcrystals (Yield: 0.12 g, 46%). M.p. 222–225 °C dec. (Found: C, 42.81; H, 2.32; $C_{46}H_{30}F_{12}O_2P_2Pt_2$ requires C, 42.67; H, 2.34%). Selected IR data (cm^{-1}): CH_2Cl_2 solution ν(C≡O) 2077vs; Nujol mull $\nu(CF)_{sym}$ 1243s, 1224s, $\nu(CF)_{deg}$ 1134s, 1122s, 1098s.

$[Pt_2(CO)_2(PBzPh_2)_2(\mu\text{-}\eta^1\text{:}\eta^1\text{-}CF_3C{\equiv}CCF_3)_2]$ (6). Prepared as for **5**, starting with $[Pt_3(CO)_3(PBzPh_2)_3]$ (0.132 g, 0.088 mmol) and $CF_3C{\equiv}CCF_3$ (43 ml, 1.79 mmol). Yield: 0.077 g (44%) as ivory microcrystals after recrystallization from dichloromethane–heptane. M.p. 215–218 °C dec. (Found: C, 43.34; H, 2.52; $C_{48}H_{34}F_{12}O_2P_2Pt_2$ requires C, 43.58; H, 2.59%). Selected IR data (cm^{-1}): CH_2Cl_2 solution ν(C≡O) 2078vs; Nujol mull $\nu(CF)_{sym}$ 1241s, 1226s, $\nu(CF)_{deg}$ 1126s, 1118s, 1103s.

Crystal structures

Crystal data for 1. A yellow crystal, of which the habitus consisted of a {110} prism and a {001} pinacoid, was mounted on a Bruker SMART CCD system equipped with Mo-Kα radiation. A hemisphere of reflections was collected as ω scans over 12 h. Lattice constants were optimized using the SAINT[21] package. $C_{42}H_{30}F_6O_2P_2Pt_2$; M/g mol^{-1}: 1132.78; crystal size/mm: 0.62 × 0.33 × 0.14; T/K: 293(2); crystal system: triclinic;

space group: $P\bar{1}$; a/Å: 14.810(3); b/Å: 15.703(3); c/Å: 18.227(4); α/°: 78.32(3); β/°: 77.49(3); γ/°: 88.93(3); V/Å^3: 4051.1(14); Z: 4; D_c/g cm^{-3}: 1.857; F(000): 2152; μ/mm^{-1}: 7.040; θ range/°: 2.44 to 27.99; reflections collected/unique: 46049/17658 [R_{int} = 0.0289]; variables: 973; R_1: 0.0262, wR_2 [$I > 2\sigma(I)$]: 0.0434.

Crystal data for 3. A yellow crystal, of which the habitus consisted of {010}, {001}, {011}, {111}, {0$\bar{1}\bar{1}$} and {0$\bar{1}$0} pinacoids, was mounted on a Stoe IPDS system equipped with Mo-Kα radiation. A crystal–image plate distance of 60 mm was used and 240 images, in oscillation steps of 1°, were exposed for 3 min each. After inspection of reciprocal space, it was ascertained that the diffraction figure consisted essentially of the spots corresponding to the cell given below. For the integration, a mosaic spread of 0.008 and spot sizes between 13 and 27 pixels were used. $C_{42}H_{66}F_6O_2P_2Pt_2$; M/g mol^{-1} 1169.07; T/K: 293(2); crystal system: monoclinic; space group: $P2_1/n$; a/Å: 16.8390(11); b/Å: 15.3101(10); c/Å: 18.6194(12); β/°: 108.481(1); V/Å^3: 4552.7(5); Z: 4; D_c/g cm^{-3}: 1.706; F(000): 2296; μ/mm^{-1}: 6.266; θ range/°: 1.42 to 23.29; reflections collected/unique: 17087/6484 [R_{int} = 0.0212]; variables: 488; R_1: 0.0207, wR_2 [$I > 2\sigma(I)$]: 0.0426.

Crystal data for 6. A pale yellow crystal, of which the habitus consisted of a {110} prism, a {100} pinacoid, and (03$\bar{4}$), (0$\bar{5}\bar{6}$) and ($\bar{1}$05) pedions, was mounted on a Stoe IPDS system equipped with Mo-Kα radiation. A crystal–image plate distance of 60 mm was used and 164 images, in oscillation steps of 1°, were exposed for 5 min each. After inspection of reciprocal space, it was ascertained that the diffraction figure consisted essentially of the spots corresponding to the cell given below. For the integration, a mosaic spread of 0.007 and spot sizes between 13 and 19 pixels were used. $C_{48}H_{34}F_{12}O_2P_2Pt_2$; M/g mol^{-1}: 1322.87; T/K: 293(2); crystal system: monoclinic; space group: $P2_1/c$; a/Å: 13.001(3); b/Å: 13.740(3); c/Å: 26.580(5); β/°: 104.03(3); V/Å^3: 4606(2); Z: 4; D_c/g cm^{-3}: 1.908; F(000): 2528; μ/mm^{-1}: 6.224; θ range/°: 2.46 to 28.06; reflections collected/unique: 35396/10541 [R_{int} 0.0298]; variables: 646; R_1: 0.0270, wR_2: [$I > 2\sigma(I)$] 0.0402.

For all measurements, intensities were corrected for Lorentz and polarization effects. An absorption correction based on the crystal habiti were computed with the help of the XPREP[22] program. The decay during the measurements was negligible. The structures were solved with the help of DIRDIF-96,[23] and refined by means of SHELXTL 5.05.[22] All non-hydrogen atoms were refined anisotropically, and all hydrogens, which were made to ride on their associated carbons, isotropically.

CCDC reference numbers 183074–183076.

See http://www.rsc.org/suppdata/dt/b2/b203075f/ for crystallographic data in CIF or other electronic format.

Acknowledgements

We thank the Swiss National Science Foundation and Murst Cofin-2001 for financial support.

References

1 F. R. Hartley, *Angew. Chem., Int. Ed. Engl.*, 1972, **11**, 596.
2 F. G. A. Stone, *Acc. Chem. Res.*, 1981, **14**, 318.
3 G. B. Young, in *Comprehensive Organometallic Chemistry II*, ed. E. W. Abel, F. G. A. Stone and G. Wilkinson, Pergamon, Oxford, 1995, vol. 9, p. 533.
4 N. M. Boag, M. Green and F. G. A. Stone, *J. Chem. Soc., Chem. Commun.*, 1980, 1281.
5 N. M. Boag, M. Green, J. A. K. Howard and F. G. A. Stone, *J. Chem. Soc., Dalton Trans.*, 1991, 862.
6 G. J. Spivak and R. J. Puddephatt, *J. Organomet. Chem.*, 1998, **551**, 383.
7 (*a*) D. M. Hoffman, R. Hoffman and C. R. Fisel, *J. Am. Chem. Soc.*, 1982, **104**, 3858; (*b*) D. M. Hoffman and R. Hoffman, *J. Chem. Soc., Dalton Trans.*, 1982, 1471, and references therein.
8 R. Ros, A. Tassan, G. Laurenczy and R. Roulet, *Inorg. Chim. Acta*, 2000, **303**, 94.
9 R. Ros, G. Facchin, A. Tassan, R. Roulet, G. Laurenczy and F. Lukas, *J. Cluster Sci.*, 2001, **12**(1), 99.
10 R. Ros, A. Tassan, R. Roulet, V. Duprez, S. Detti, G. Laurenczy and K. Schenk, *J. Chem. Soc., Dalton Trans.*, 2001, 2858.
11 A. Moor, P. S. Pregosin and L. M. Venanzi, *Inorg. Chim. Acta*, 1981, **48**, 153.
12 D. Carbona, R. Thouvenot, L. M. Venanzi, F. Bachechi and L. Zambonelli, *J. Organomet. Chem.*, 1983, **250**, 589.
13 H. Rüegger and D. Moskau, *Magn. Reson. Chem.*, 1991, **29**, 511.
14 B. W. Davies and N. C. Payne, *Inorg. Chem.*, 1974, **13**, 1848.
15 J. F. Richardson and N. C. Payne, *Can. J. Chem.*, 1977, **55**, 3203.
16 D. H. Farrar and N. C. Payne, *J. Organomet. Chem.*, 1981, **220**, 239.
17 *Spec. Publ. Chem. Soc.*, 1965, **18**, S16s.
18 G. K. Anderson, in *Comprehensive Organometallic Chemistry II*, ed. E. W. Abel, F. G. A. Stone, and G. Wilkinson, Pergamon, Oxford, 1995, vol. 9, p. 445.
19 J. Chatt and P. Chini, *J. Am. Chem. Soc.*, 1970, 1538.
20 K. H. Dalmer, A. Moor, R. Naegli and L. M. Venanzi, *Inorg. Chem.*, 1991, **30**, 4285.
21 SAINT, Programme for the Reduction of Data from an Area Detector, version 4.05, Bruker Analytical X-Ray Instruments, Inc, Madison, WI, USA, 1996.
22 G. M. Sheldrick, SHELXTL 5.05, Bruker Analytical X-Ray Instruments, Inc, Madison, WI, USA, 1996.
23 P. T. Beurskens, G. Beurskens, W. P. Bosman, R. de Gelder, S. García-Granda, R. O. Gould, R. Israël and M. M. Smits, The DIRDIF-96 System of Programmes, Laboratorium voor Kristallografie, Katholieke Universiteit Nijmegen, 1996.